Fibrillin-1 and -2 differentially modulate endogenous TGF-β and BMP bioavailability during bone formation

Harikiran Nistala,[1] Sui Lee-Arteaga,[1] Silvia Smaldone,[1] Gabriella Siciliano,[1] Luca Carta,[1] Robert N. Ono,[2,3] Gerhard Sengle,[2,3] Emilio Arteaga-Solis,[4] Regis Levasseur,[5] Patricia Ducy,[5] Lynn Y. Sakai,[2,3] Gerard Karsenty,[5] and Francesco Ramirez[1]

[1]Department of Pharmacology and Systems Therapeutics, Mount Sinai School of Medicine, New York, NY 10021
[2]Shriners Hospital for Children and [3]Department of Biochemistry and Molecular Biology, Oregon Health and Science University, Portland, OR 97239
[4]Division of Pulmonary Medicine, Department of Pediatrics and [5]Department of Development and Genetics, College of Physicians and Surgeons, Columbia University, New York, NY 10029

Extracellular regulation of signaling by transforming growth factor (TGF)–β family members is emerging as a key aspect of organ formation and tissue remodeling. In this study, we demonstrate that fibrillin-1 and -2, the structural components of extracellular microfibrils, differentially regulate TGF-β and bone morphogenetic protein (BMP) bioavailability in bone. Fibrillin-2–null (*Fbn2*$^{-/-}$) mice display a low bone mass phenotype that is associated with reduced bone formation in vivo and impaired osteoblast maturation in vitro. This *Fbn2*$^{-/-}$ phenotype is accounted for by improper activation of latent TGF-β that selectively blunts expression of osterix, the transcriptional regulator of osteoblast maturation, and collagen I, the structural template for bone mineralization. Cultured osteoblasts from *Fbn1*$^{-/-}$ mice exhibit improper latent TGF-β activation as well, but mature faster because of increased availability of otherwise matrix-bound BMPs. Additional in vitro evidence excludes a direct role of microfibrils in supporting mineral deposition. Together, these findings identify the extracellular microfibrils as critical regulators of bone formation through the modulation of endogenous TGF-β and BMP signaling.

Introduction

33 TGF-β–related proteins orchestrate a broad spectrum of developmental and physiological processes in mammals (Katagiri et al., 2008). Multiple mechanisms that operate within and outside the cell and at the cell surface regulate signaling by TGF-β family members in a context-specific manner (Shi and Massagué, 2003; ten Dijke and Arthur, 2007; Kang et al., 2009). Extracellular control of endogenous (local) TGF-β signaling, in particular, is emerging as an important aspect of organ formation and tissue homeostasis (Ramirez and Rifkin, 2009). TGF-β1, -2, and -3 (hereafter collectively referred to as TGF-β) are secreted either as a small latent complex (SLC) in which the bioactive homodimer remains associated with the processed propeptides (latency-associated protein [LAP]) or as a large latent complex (LLC) in which the SLC is bound to latent TGF-β–binding proteins (LTBPs) 1, 3, or 4 (Annes et al., 2003). LAP association blocks ligand interaction with TGF-β receptors, whereas LTBP binding targets the SLC to the ECM through LTBP-mediated association with fibronectin or fibrillin assemblies (microfibrils). Several extracellular molecules (many of which interact with microfibrils) and integrin receptors are involved in releasing TGF-β from the ECM, disrupting LAP-mediated latency, or inhibiting TGF-β activity. Bone morphogenetic proteins (BMPs), too, are secreted and targeted to the ECM as C-terminal disulfide cross-linked dimers that are noncovalently associated

Correspondence to Francesco Ramirez: francesco.ramirez@mssm.edu
R. Levasseur's present address is Angers University Hospital, Angers 49933, France.

Abbreviations used in this paper: BFR, bone formation rate; BMP, bone morphogenetic protein; BV, bone volume; CCA, congenital contractural arachnodactyly; cOb, calvarial osteoblast; LAP, latency-associated protein; LLC, large latent complex; LTBP, latent TGF-β–binding protein; μCT, microcomputed tomography; MFS, Marfan syndrome; MSC, marrow stromal cell; OS, osteoinductive supplement; qPCR, quantitative real-time RT-PCR; SLC, small latent complex; TV, total volume; WT, wild type.

The Rockefeller University Press $30.00
J. Cell Biol. Vol. 190 No. 6 1107–1121
www.jcb.org/cgi/doi/10.1083/jcb.201003089

with the N-terminal propeptides (Katagiri et al., 2008). However, in contrast to TGF-β, in vitro bioactivity assays suggest that BMP prodomains generally may not confer latency to the associated dimers (Sengle et al., 2008a). Moreover, the factors and mechanisms that control BMP sequestration in and release from the ECM are less well understood than those regulating TGF-β bioavailability. Earlier characterization of a limb-patterning defect (syndactyly) in mice with inactivated fibrillin-2 gene (*Fbn2*) expression revealed a genetic interaction between this ECM molecule and BMP7 signaling in the forming autopods (Arteaga-Solis et al., 2001). Subsequent in vitro experiments demonstrated that BMP prodomains can directly interact with the N termini of fibrillin-1 and -2 (Sengle et al., 2008b).

Fibrillin microfibrils are ubiquitous architectural elements of the ECM that endow connective tissues with specific physical properties, either as obligatory constituents of elastic fibers or as elastin-free assemblies (Ramirez and Rifkin, 2009). Fibrillins interact with several ECM proteins during microfibril biogenesis, and many of these interactions occur at or near the same sites of LLC and BMP binding (Ramirez and Sakai, 2010). The pleiotropic manifestations of Marfan syndrome (MFS; OMIM-154700) and congenital contractural arachnodactyly (CCA; OMIM-121050), which are caused by mutations in fibrillin-1 and -2, respectively, underscore the importance of fibrillin microfibrils in the formation and function of several organ systems (Ramirez and Dietz, 2007). Moreover, the distinct phenotypes of MFS and CCA imply that fibrillin-1 and -2 have discrete functions in spite of them being the building blocks of the same matrix assemblies. Consistent with this postulate, $Fbn1^{-/-}$ mice do not share the limb-patterning defect of $Fbn2^{-/-}$ mice that was genetically associated with low BMP7 signaling (Arteaga-Solis et al., 2001; Carta et al., 2006), and aortic wall homeostasis is severely impaired only in *Fbn1* mutant mice largely as a result of promiscuous TGF-β signaling (Pereira et al., 1999; Judge et al., 2004; Habashi et al., 2006). Thus, fibrillin-1 and -2 may control local TGF-β and BMP bioavailability differently, depending on the organ system, developmental stage, or physiological program.

The scope of this study was to test the aforementioned hypothesis using bone formation as an informative model system because of the following considerations. First, osteogenesis is a fairly well understood process that can be replicated in vitro using primary osteoblast cultures (Stein et al., 1990; Karsenty et al., 2009). Second, TGF-β and BMPs are abundantly stored in the bone matrix from which they are released in a timely fashion and at the appropriate concentration to regulate osteogenic differentiation (Rosen and Thies, 1992; Mundy et al., 1995; Katagiri et al., 2008). Third, *Fbn1* and *Fbn2* are highly expressed in the progenitor and differentiating osteoblasts of forming and adult bones (Zhang et al., 1994, 1995; Kitahama et al., 2000; Arteaga-Solis et al., 2001; Quondamatteo et al., 2002; Roman-Roman et al., 2003; Ulloa-Montoya et al., 2007). Fourth, low bone mass (osteopenia) is one of the few clinical manifestations in common between MFS and CCA patients (Ramirez and Arteaga-Solis, 2008). Our experiments demonstrate that fibrillin-2 and -1 regulate osteoblast maturation by controlling TGF-β bioavailability and calibrating TGF-β and BMP levels, respectively. Furthermore, they exclude a direct contribution of microfibrils to the formation of the organic substrate that supports mineral deposition in bone. Collectively, these findings significantly advance our understanding of the extracellular control of local TGF-β and BMP signaling in bone physiology.

Results

Loss of fibrillin-2 leads to decreased bone mass

$Fbn2^{-/-}$ mice are viable and fertile but proportionally smaller than wild-type (WT) littermates throughout life and irrespective of gender (Arteaga-Solis et al., 2001). Consistent with this last observation, a modest but statistically significant ($P < 0.003$) length reduction (4.5%) was recorded in 4-mo-old $Fbn2^{-/-}$ femurs compared with WT counterparts ($n = 10$ for each genotype). Additionally, morphometric analyses of mid-diaphyseal cross sections of 1-mo-old mutant femurs identified changes in bone shape that were appreciably more evident in 4-mo-old $Fbn2^{-/-}$ mice. Changes in the latter set of mutant femurs included a 15% smaller bone width ($P < 0.0003$) and a 25% narrower marrow cavity than WT specimens ($n = 7$). In contrast, 4-d-old (postnatal day [P] 4) *Fbn2*-null femurs were normally shaped and displayed morphologically unremarkable growth plates (unpublished data), implying a probable defect in postnatal bone modeling rather than an abnormality in endochondral bone development.

Consistent with the aforementioned prediction, microcomputed tomography (μCT) and histomorphometric analyses detected an appreciable deficit of cancellous bone in 3- and 6-mo-old mutant vertebrae. To be specific, examination of the former samples ($n = 5$) revealed a 58% decrease in bone mineral density (bone mineral content/total volume [TV]; $P = 0.0007$), a 27% decrease in bone mass (bone volume [BV]/TV; $P = 0.0008$; Fig. 1 A), and 52% fewer trabeculae ($P < 0.003$) and 66% greater intertrabecular space ($P < 0.01$). Parallel in vivo analyses showed a 55% reduction in bone formation rate (BFR; $n = 6$; $P = 0.0003$) associated with a seemingly normal complement of osteoblasts (number of surface osteoblasts/bone perimeter; $n = 5$; $P = 0.24$) in mutant compared with WT mice (Fig. 1 B). Altogether, these static and dynamic assessments strongly suggested that impaired bone formation is a major determinant of osteopenia in $Fbn2^{-/-}$ mice.

Loss of fibrillin-2 impairs osteoblast maturation

In line with the in vivo data, *Fbn2*-null calvarial osteoblasts (cObs) or marrow stromal cells (MSCs) cultured with osteoinductive supplements (OSs) yielded fewer and smaller mineralized nodules than the WT counterparts (Fig. 2 A). Impaired osteoblast maturation is characterized by a progressively modest reduction in AP activity (Fig. 2 B) and by an appreciable decrease in collagen deposition (as visualized by van Gieson counterstaining of mutant cOb cultures; Fig. 2 A). Quantitative real-time RT-PCR (qPCR) assays confirmed a substantial downregulation of α2(I) collagen (*Col1a2*) and osteocalcin (*Bglap1*; a marker of terminal osteoblast differentiation) in mutant cOb in

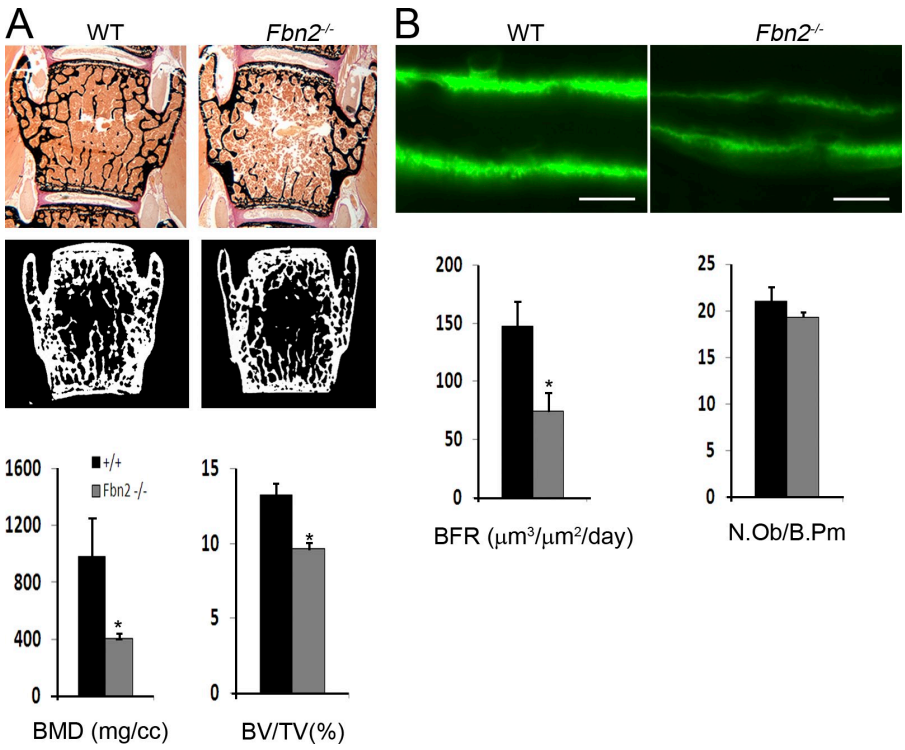

Figure 1. **Reduced bone mass and BFR in *Fbn2*$^{-/-}$ mice.** (A) Representative von Kossa staining and μCT images of vertebral sections from 3-mo-old WT and *Fbn2*$^{-/-}$ male mice with histograms summarizing the μCT measurements of volumetric bone mineral density (BMD) and BV/TV in these samples. (B) Illustrative examples of dual-calcein labeling in tibiae of 3-mo-old WT and *Fbn2*$^{-/-}$ male mice with histograms summarizing BFR values and osteoblast numbers in WT and mutant samples. Error bars indicate mean ± SD, and asterisks indicate statistically significant differences ($P < 0.05$) between genotypes. Bars, 50 μm.

addition to excluding a compensatory up-regulation of *Fbn1* (Fig. 2 C). The qPCR assays also correlated impaired maturation of *Fbn2*-null cOb cultures with lower than normal activity of the osterix gene (*Osx*), which encodes a transcriptional regulator of osteoblast differentiation (Nakashima et al., 2002), and with unremarkable levels of *Runx2* mRNA, which encodes the transcriptional determinant of osteoprogenitor commitment (Fig. 2 C; Ducy et al., 1997). Identical results were obtained with RNA purified from the calvariae of *Fbn2*$^{-/-}$ newborns (Fig. 2 C). Lastly, no significant differences in cell proliferation, BrdU incorporation, and *C-myc* and *Ccnd1* (cyclin D1) mRNA levels were noted between mutant and WT cOb cultures 3 d before and at the time of OS treatment (Fig. 2, D and E). Similar results were obtained by comparing cell survival and apoptosis of mutant and control cOb cultures (Fig. 2, F and G).

In vivo and ex vivo cell-marking experiments confirmed the aforementioned maturation defect by showing a substantial reduction in the number of GFP-positive cells in neonatal bones and cOb cultures from *Fbn2*$^{-/-}$ mice harboring the *pOBCol2.3GFP* transgene, which is specifically activated during osteoblast maturation (Fig. 3; Kalajzic et al., 2005). Incidentally, GFP marking confirmed that fewer surface osteoblasts are actively producing collagen I in mutant bones (Fig. 3 B). Likewise, fewer GFP-positive cells in cOb cultures from *Fbn2*$^{-/-}$ mice harboring the *Osx1-GFP::Cre* transgene reiterated the negative impact of the mutation on this critical regulator of osteoblast maturation (Fig. 3 C). Importantly, however, the finding that *Fbn2*-null cOb cultures can respond to the osteoinductive signal of exogenously added BMP2 by restoring *Osx* and *Col1a2* activity and improving mineral nodule formation demonstrated the reversible nature of the cell defect (Fig. 3 D). Incidentally, the ∼10% greater maturation of BMP2-treated compared with untreated WT cOb was not statistically significant because of an outlier in the latter set of samples (Fig. 3 D). This point notwithstanding, we concluded that loss of fibrillin-2 delays osteoblast maturation by selectively interfering, presumably in an osterix-dependent manner, with the differentiation program that normally promotes maturation and mineralization of the bone ECM.

Latent TGF-β is improperly activated in *Fbn2*-null osteoblast cultures

Previous evidence implicating fibrillin-1 in the extracellular control of TGF-β signaling (Isogai et al., 2003; Neptune et al., 2003) prompted us to investigate whether fibrillin-2 is involved in this regulatory process as well. To this end, interactions between fibrillin-2 and LTBPs 1 and 4 were first evaluated in vitro using surface plasmon resonance and recombinant peptides that correspond to the N-terminal segment of fibrillin-2 (rF86) and the C-terminal sequences of LTBPs 1 and 4 (L1K and L4K). The BIAcore assays established that the rF86 fragment binds the L1K and L4K peptides with the same high affinity (K_d = 20–25 nM), as previously shown for the corresponding N-terminal segment of fibrillin-1 (Fig. 4 A; Ono et al., 2009). Next, *Fbn2*-null cObs were found to display a greater ALK5-dependent nuclear accumulation of pSmad2 (phosphorylated Smad2) than WT cells (Fig. 4 B). Furthermore, relative levels of pSmad2/3 proteins and transcriptional activity of a transfected TGF-β–inducible plasmid (p3TP-lux) were both appreciably higher in mutant than control cells (Fig. 4 C and Fig. S1 A). Lastly, the TMLC bioassay (epithelial cells stably transfected with p3TP-lux; Abe et al., 1994) revealed more active TGF-β but nearly normal amounts of total TGF-β in *Fbn2*-null compared with WT cOb cultures (Fig. 4 D). The latter finding was independently supported by qPCR analyses showing normal steady-state levels of *Tgf-β* transcripts in *Fbn2*-null osteoblasts (Fig. 4 E).

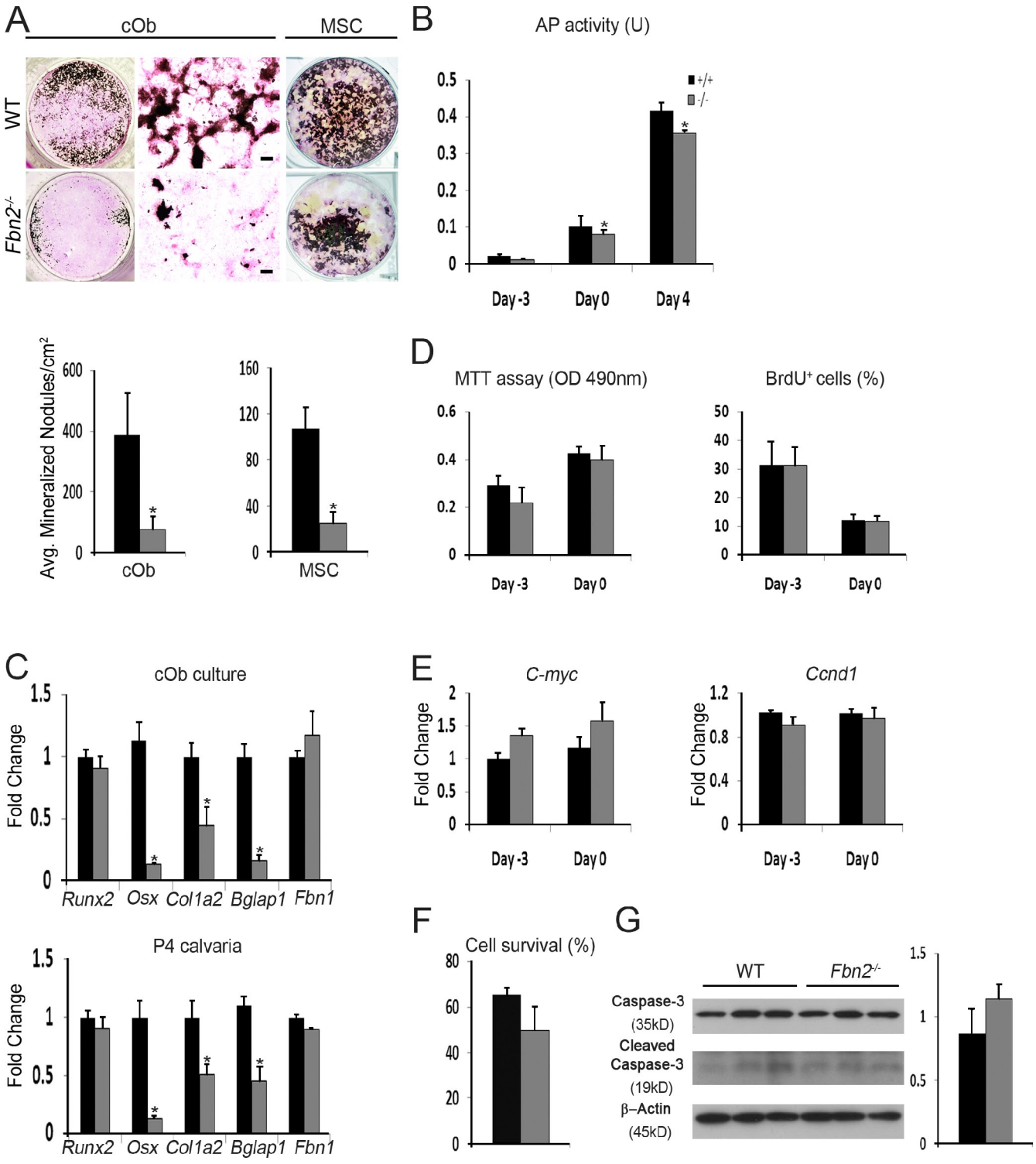

Figure 2. **Impaired maturation of *Fbn2*-null osteoblasts.** (A) Illustrative images of von Kossa staining of neonatal cOb (left) and adult MSCs (right) along with magnified van Geison–counterstained images (middle) of cOb differentiated for 21 d after OS administration. Histograms summarize the number of mineralized nodules in WT and *Fbn2*-null (*Fbn2*$^{-/-}$) cOb (n = 15) and MSC (n = 5) cultures. Bars, 200 µm. (B) AP activity of WT and *Fbn2*$^{-/-}$ cOb measured 3 d before (day −3) and 4 d after (day 4) OS administration (day 0) and normalized to total protein levels (n = 5). (C) qPCR estimates of indicated transcripts in total RNA isolated from day 4 cOb cultures (n = 4; top) or P4 calvariae of WT and *Fbn2*$^{-/-}$ mice (n = 4; bottom). (D and E) MTT and BrdU incorporation assays (D) and *C-myc* and *Ccnd1* mRNA levels (E) at the indicated days of cOb differentiation (n = 6). (F and G) Cell survival evaluated by Trypan blue exclusion (F; n = 4) and cell apoptosis (G) measured as the fraction of cleaved caspase-3 over full-length protein (with histograms representing densitometric analyses) in WT and mutant cObs. Error bars indicate mean ± SD, and asterisks indicate statistically significant differences ($P < 0.05$) between genotypes.

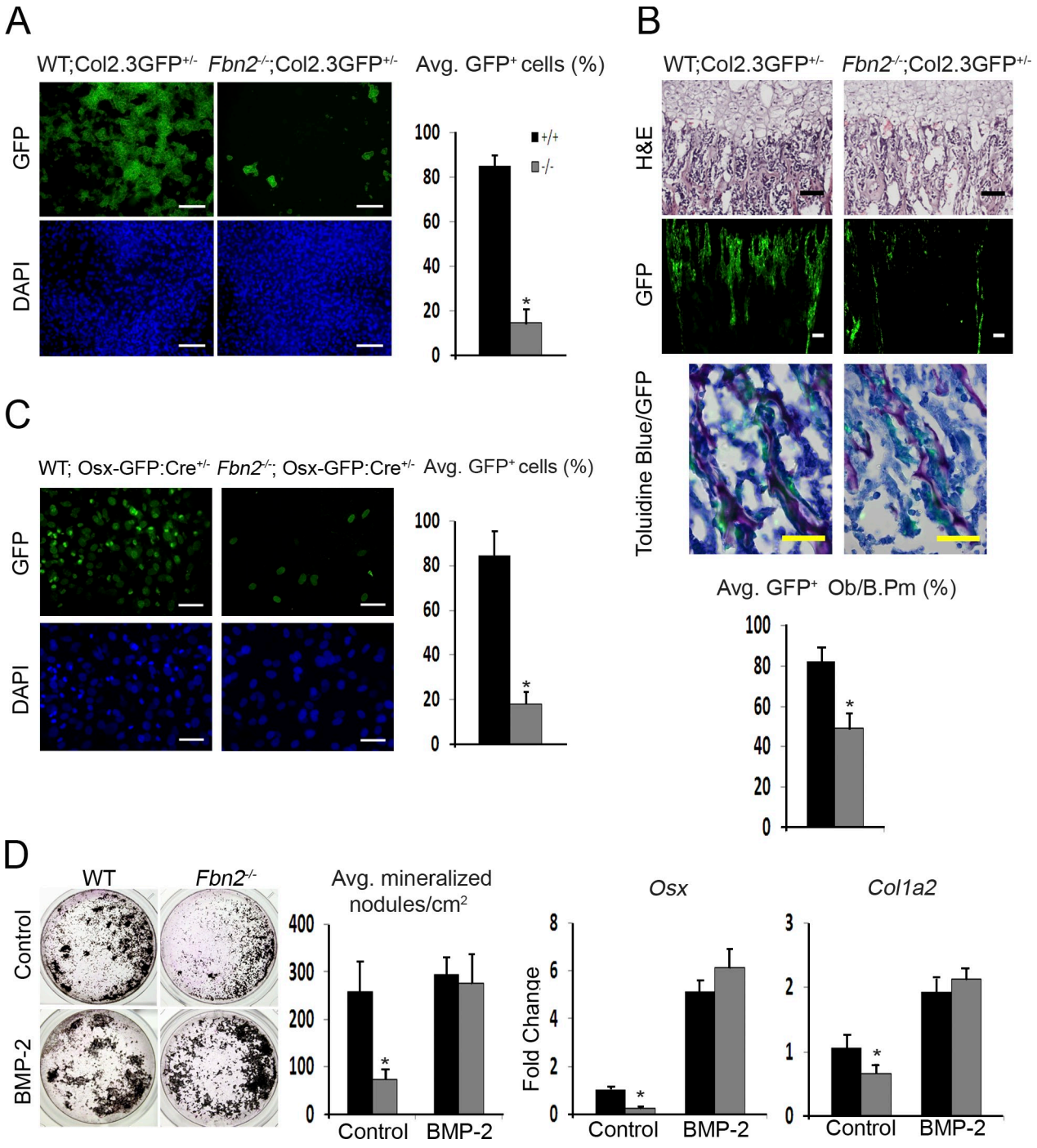

Figure 3. **Osterix and collagen down-regulation in *Fbn2*-null osteoblasts.** (A and C) Illustrative images of *pOBCol2.3GFP* (A) or *Osx-GFP::Cre* transgene expression (C) in *Fbn2*-null and WT cOb at day 17 or 4 of differentiation, respectively, with histograms summarizing the number of GFP-positive cells ($n = 3$); nuclei are DAPI stained. (B) Illustrative images of tibiae of $Fbn2^{-/-}$ and WT mice harboring the *pOBCol2.3GFP* transgene that include (from top to bottom) hematoxylin/eosin staining, GFP expression, and magnified views of toluidine- and GFP-positive cells; histograms summarize cell counts in the last images ($n = 3$). (D) von Kossa staining after 21 d of differentiation of cOb treated with or without 100 ng/ml rhBMP2 with histograms (right) summarizing numbers of mineralized nodules and levels of *Osx* and *Col1a2* transcripts in mutant and WT samples ($n = 3$). Error bars indicate mean ± SD, and asterisks indicate statistically significant differences ($P < 0.05$) between genotypes. Bars: (A and B [middle]) 100 µm; (B [top and bottom] and C) 50 µm.

Because LTBPs target TGF-β to microfibrils (Isogai et al., 2003), we examined LTBP1 incorporation in the matrix laid down by overconfluent cOb cultures and found less immunoreactive material in *Fbn2*-null than WT cultures (Fig. 5 A). TMLC bioassays correlated this visual finding with an ∼47% decrease in the amount of TGF-β extracted from the matrix (relative to the amount extracted from cells) of mutant compared with WT samples ($n = 3$; $P < 0.0001$). Furthermore, qPCR analyses showed that *Ltbp1* mRNA accumulation in differentiating mutant cOb (time points at days 0, 3, and 7 of osteoinduction) is less than control (∼14%) only 3 d after OS treatment ($n = 3$; $P < 0.046$). Taken at face value, these results strongly suggested

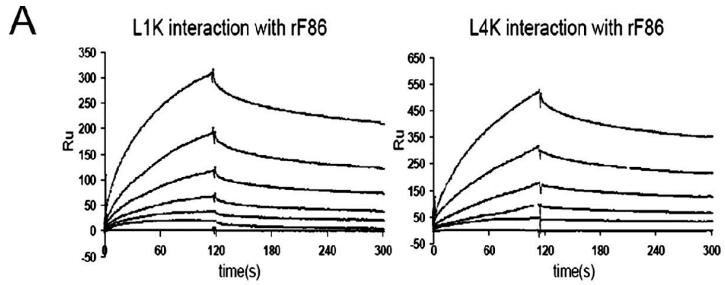

Interaction Ligand/Analyte	k_{on}[1/M*s]/k_{off}[1/s]	K_D[nM]
L1K/rF86	4.29×10^{4} / 8.78×10^{-4}	2.05×10^{-8}
L4K/rF86	4.94×10^{4} / 1.25×10^{-3}	2.53×10^{-8}

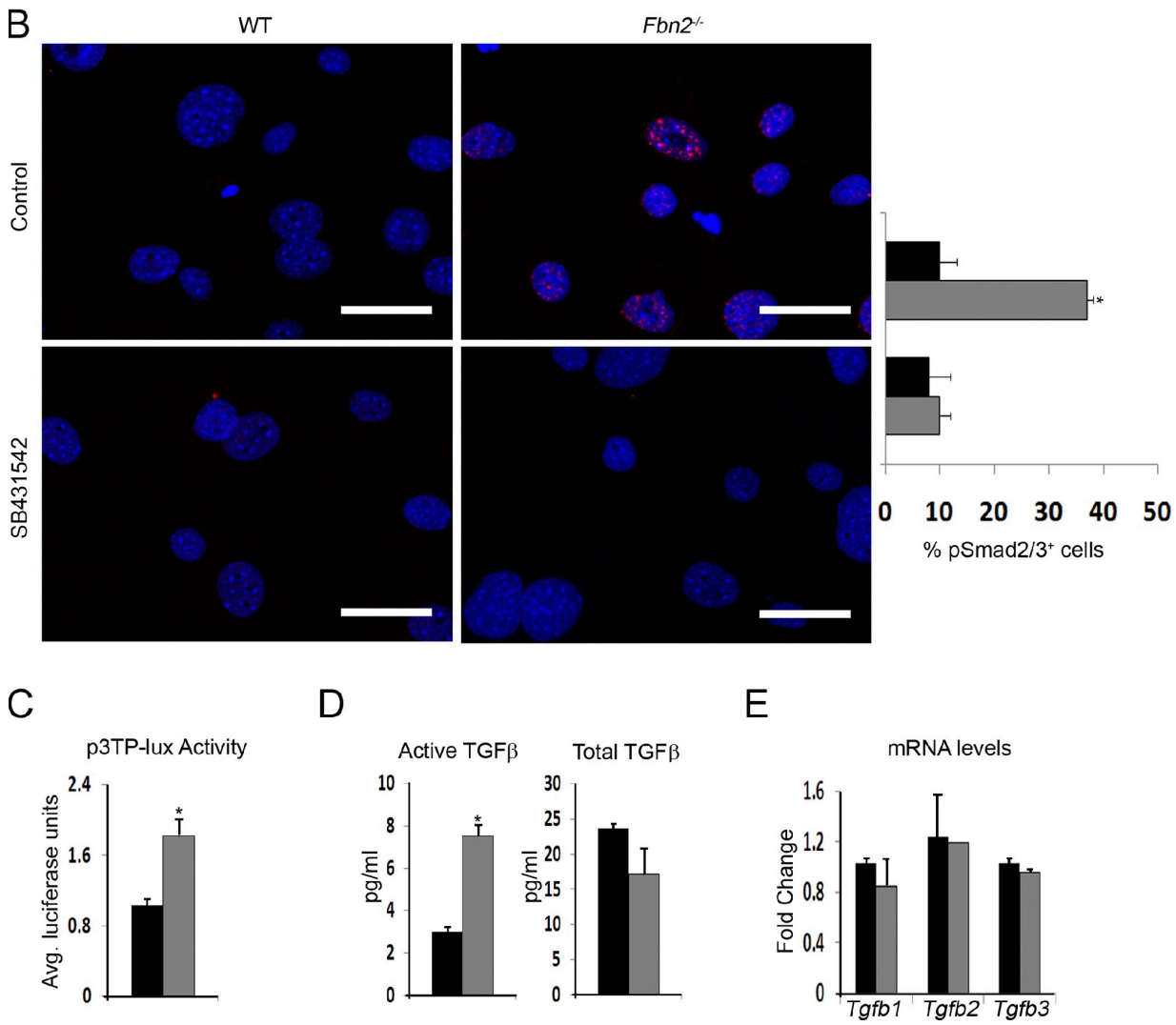

Figure 4. **Fibrillin-2 controls TGF-β bioavailability.** (A) Surface plasmon resonance sensograms of binding of immobilized L1K (left) and L4K (right) to rF86 at concentrations between 0 (baseline tracing) and 200 nM (top tracing). Binding was recorded as resonance units (RU), and nonspecific binding to control surface was subtracted at a molar ratio of 1:1. The table summarizes the affinity data (expressed as K_d) for interactions between the LTBPs and fibrillin-2 peptide. (B) Immunodetection of nuclear pSmad2 accumulation in day 4 cOb cultured in low serum with or without SB431542; nuclei are DAPI stained. Histograms summarize the percentage of pSmad2-positive nuclei in WT (black) and mutant (gray) cells (n = 3). (C) Transcriptional activity of p3TP-lux reporter plasmid transfected in WT or *Fbn2*-null cOb cultured in low serum (n = 3). (D) TMLC bioassays (n = 5) measuring active TGF-β in WT or *Fbn2*-null cOb cultures (left) or total TGF-β in heat-activated conditioned media of the same cultures (right). (E) qPCR estimates of *Tgf-β* transcripts in WT and *Fbn2*-null cOb (n = 3). Error bars indicate mean ± SD, and asterisks indicate statistically significant differences ($P < 0.05$). Bars, 50 µm.

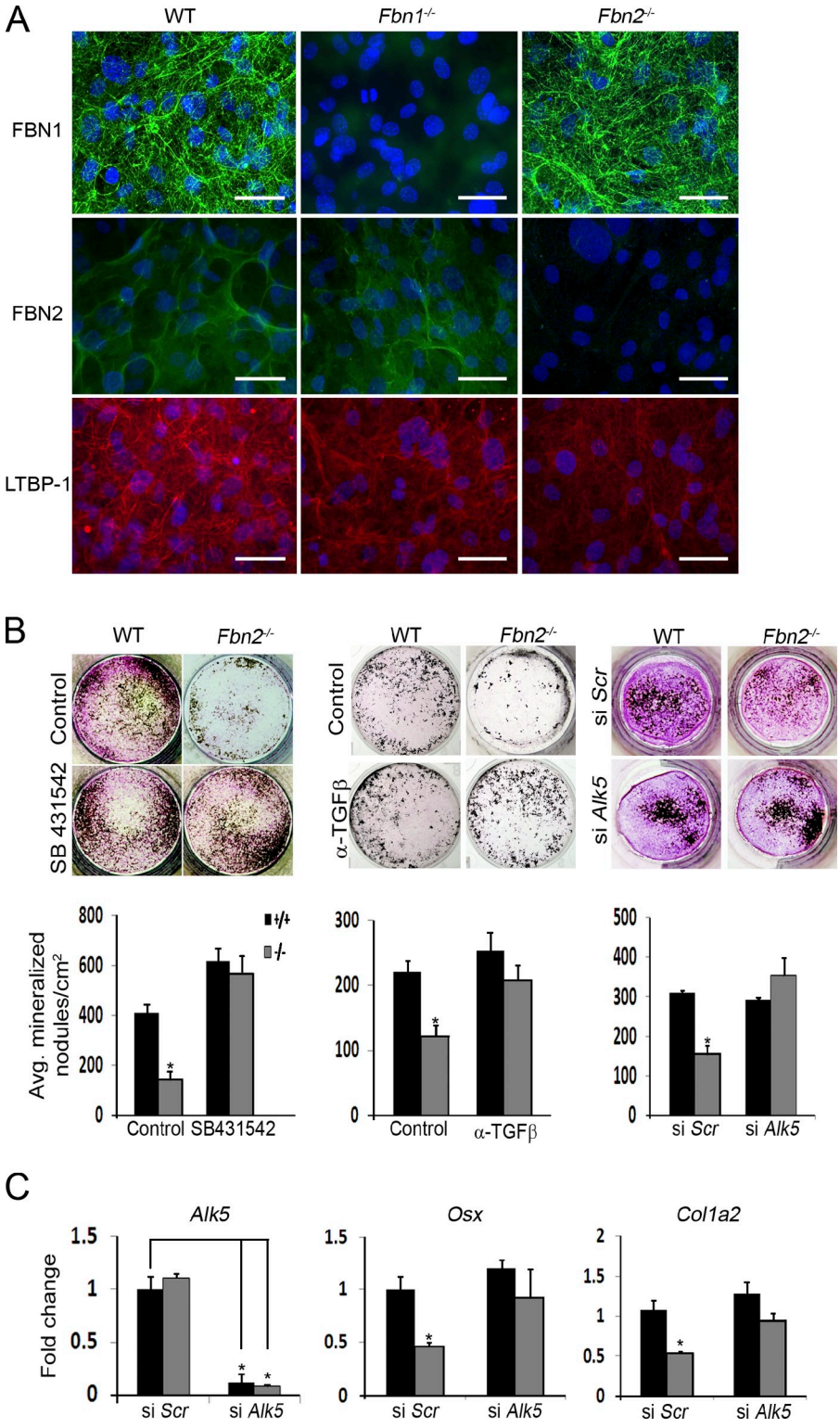

Figure 5. **Elevated TGF-β signaling limits *Fbn2*-null osteoblast maturation.** (A) Illustrative images of immunoreactive material corresponding to the indicated proteins deposited in the ECM of overconfluent WT, *Fbn1*-null, and *Fbn2*-null cOb cultures after 4 d of differentiation; nuclei are DAPI stained. Bars, 50 µm. (B) Maturation of WT and *Fbn2*-null cOb cultures treated with 1 µM SB431542, 300 ng/ml neutralizing pan–TGF-β antibody, or 50 µM *Alk5* siRNA with histograms summarizing the number of mineralized nodules in each treatment (n = 3). (C) qPCR estimates of the indicated mRNA levels in the *Alk5* silencing experiments. Error bars indicate mean ± SD, and asterisks indicate statistically significant differences ($P < 0.05$).

that loss of fibrillin-2 promotes improper TGF-β activation mostly by impairing LLC sequestration in the osteoblast matrix. Decreased matrix incorporation of LTBP1 in the presence of robust *Fbn1* expression further suggested that fibrillin-1 could not compensate for the loss of fibrillin-2 deposition in differentiating cOb cultures. This last observation is analogous to the previous finding that the BMP-dependent syndactyly of $Fbn2^{-/-}$ mice is not seen in $Fbn1^{-/-}$ mice even though both proteins are abundantly deposited in the ECM of the forming autopods (Arteaga-Solis et al., 2001; Carta et al., 2006).

To test the postulated involvement of improper TGF-β signaling, mineral nodule formation was assessed in *Fbn2*-null cOb cultures that were induced to differentiate in the presence of either an ALK5 kinase inhibitor or a pan–TGF-β–neutralizing antibody or that were transfected with siRNA against *Alk5* before OS treatment. Inhibition of TGF-β signaling by any of

these three strategies equally improved maturation of *Fbn2*-null cOb (Fig. 5 B). Phenotypic rescue of *Alk5*-silenced mutant cOb was further associated with normalization of *Osx* and *Col1a2* transcript levels (Fig. 5 C). These results were therefore interpreted to indicate that improper activation of latent TGF-β secondary to loss of fibrillin-2 impairs bone formation by interfering specifically with the ability of osteoblasts to assemble a mineralization-competent bone matrix. Normal TGF-β signaling in another microfibril-rich tissue (skin) and fibrillin-producing cells (dermal fibroblasts) of *Fbn2*$^{-/-}$ mice indirectly validated the specific effect of the mutation in osteoblasts and bone (unpublished data).

TGF-β and BMP signaling are both abnormally high in *Fbn1*-null osteoblasts

Although neonatal lethality of *Fbn1*$^{-/-}$ mice limits performing extensive analyses of bone formation (Carta et al., 2006), these mutant animals nonetheless enabled us to compare and contrast osteogenic differentiation on a matrix deficient for either fibrillin-1 or -2. *Fbn1*-null cOb proliferated normally but, in contrast to *Fbn2*-null cells, they yielded more mineral nodules than WT cultures (Fig. 6, A and B); they also displayed a modest increase in *Osx* expression, a significant up-regulation of *Col1a2* and *Bglap1*, and normal *Runx2* and *Fbn2* activity (Fig. 6 C). In vivo levels of *Col1a2* and *Bglap1* (but not *Osx*) transcripts were appreciably higher than control, and collagen accumulation was slightly greater in mutant than WT bones (Fig. 6 D and Fig. S1 C). Moreover, AP-positive cells and mineral deposits appeared earlier and grew faster in *Fbn1*-null than WT cOb cultures (Fig. S1 D). Collectively, these observations were consistent with the notion that loss of fibrillin-1 accelerates osteoblast maturation.

Similar to *Fbn2*-null cells, *Fbn1*-null cOb cultures displayed less LTBP1-immunoreactive material, more activated TGF-β, and greater p3TP-lux activity than WT cultures (Fig. 5; and Fig. 6, E and F). Normal amounts of total TGF-β and normal levels of *Tgf-β* transcripts further corroborated the notion that loss of fibrillin-1 deposition leads to improper activation of latent TGF-β complexes (Fig. 6, E and G). Additionally, normal responses of *Fbn1*-null cOb cultures to the opposing signals of recombinant TGF-β1 and BMP2 excluded possible changes of cell identity (Fig. S1 E). These findings raised the question of which factors may be responsible for overriding the negative impact of heightened TGF-β signaling on osteoblast maturation. We reasoned that BMPs were obvious candidates because they are potent osteoinductive factors that interact in vitro with fibrillin-1 (Sengle et al., 2008b).

Two sets of evidence supported our hypothesis. First, immunofluorescence microscopy documented greater accumulation of pSmad1/5/8 in the nuclei of *Fbn1*-null cOb than in those of control or *Fbn2*-null cells (Fig. 7 A). These visual data were correlated with seemingly more pSmad1/5/8 proteins and higher BRE-luc activity in *Fbn1*-null cOb cultures compared with the WT or *Fbn2*-null counterparts (Fig. 7 B and Fig. S1 B). Second, BMP bioassays revealed that conditioned media from *Fbn1*-null cOb cultures stimulate C2C12BRA reporter cells (which harbor the BMP-inducible plasmid BRE-luc; Zilberberg et al., 2007) twofold more than control or *Fbn2*-null media (Fig. 7 C). Furthermore, qPCR analyses identified no significant differences in the steady-state levels of several *Bmp* transcripts between WT and *Fbn1*- or *Fbn2*-null cOb (Fig. 7, D and E). Lastly, ELISA assays estimated that BMP levels are appreciably higher in *Fbn1*-null than WT conditioned media and appreciably lower in *Fbn1*-null compared with WT matrices (109 vs. 81 pg/ml and 827 vs. 903 pg/ml, respectively; $n = 3$; $P < 0.01$). Collectively, these results suggested that loss of fibrillin-1 deposition impairs BMP sequestration in the ECM with the consequence of increasing BMP signaling and, thus, overriding the inhibition of osteoblast maturation by promiscuous TGF-β signaling.

Although the reason why a similar elevation of BMP signaling was not observed in *Fbn2*-null osteoblasts is yet to be determined, the cell culture experiments at least clarified whether or not the increases in TGF-β and BMP signaling that characterize *Fbn1*-null cOb are causally related to each other. BMP bioassays revealed that conditioned media from *Fbn1*-null cOb cultures stimulate C2C12BRA reporter cells twofold more than those from control or *Fbn2*-null cells and that this increase can be abrogated by adding the BMP antagonist noggin to the media, but not by using conditioned media from *Fbn1*-null cOb pretreated with the ALK5 inhibitor SB431542 (Fig. 7 C). Conversely, addition of noggin to *Fbn1*-null cOb cultures transfected with p3TP-lux did not affect expression of the TGF-β–responsive reporter plasmid (Fig. 6 F). These results therefore excluded the possibility that augmented TGF-β activity in *Fbn1*-null cOb cultures stimulates BMP signaling and vice versa. An implicit corollary to this conclusion is that fibrillin-1 is directly involved in calibrating the bioavailability of both TGF-β and BMP molecules during bone formation. Moreover, dysregulated TGF-β and BMP signaling in *Fbn1*-null bones is a tissue-specific trait in that only the former signaling abnormality characterizes the aortic media and vascular smooth cell cultures of *Fbn1*$^{-/-}$ mice, and neither of them is evident in the skin or dermal fibroblast cultures of the same mutant animals (Carta et al., 2006, 2009; unpublished data).

Fibrillin microfibrils are not structural components of the mineralization-competent matrix

Although the aforementioned data implicated fibrillin-1 and -2 in the differential control of local TGF-β and BMP signals during bone formation, they did not formally exclude the possibility that microfibrils may also be required to form the organic substrate promoting ECM mineralization (Murshed et al., 2005). Accordingly, the mineralizing potential of the microfibril-deficient bone matrix was assessed by the siRNA approach to circumvent the problem of embryonic lethality of mice deficient for both fibrillins (Carta et al., 2006). To this end, maturation of *Fbn1*- or *Fbn2*-silenced WT cOb was first equated with the respective phenotypes of *Fbn1*- or *Fbn2*-null cells (Fig. 8 A). This finding further corroborated the cell (culture)-autonomous nature of the fibrillin mutations. Next, *Fbn1* silencing was shown to improve mineral nodule formation in *Fbn2*-null cOb cultures (Fig. 8 B). Mineral nodule formation in cOb cultures lacking both fibrillin proteins was therefore interpreted to exclude a major structural role of microfibrils in directly supporting bone

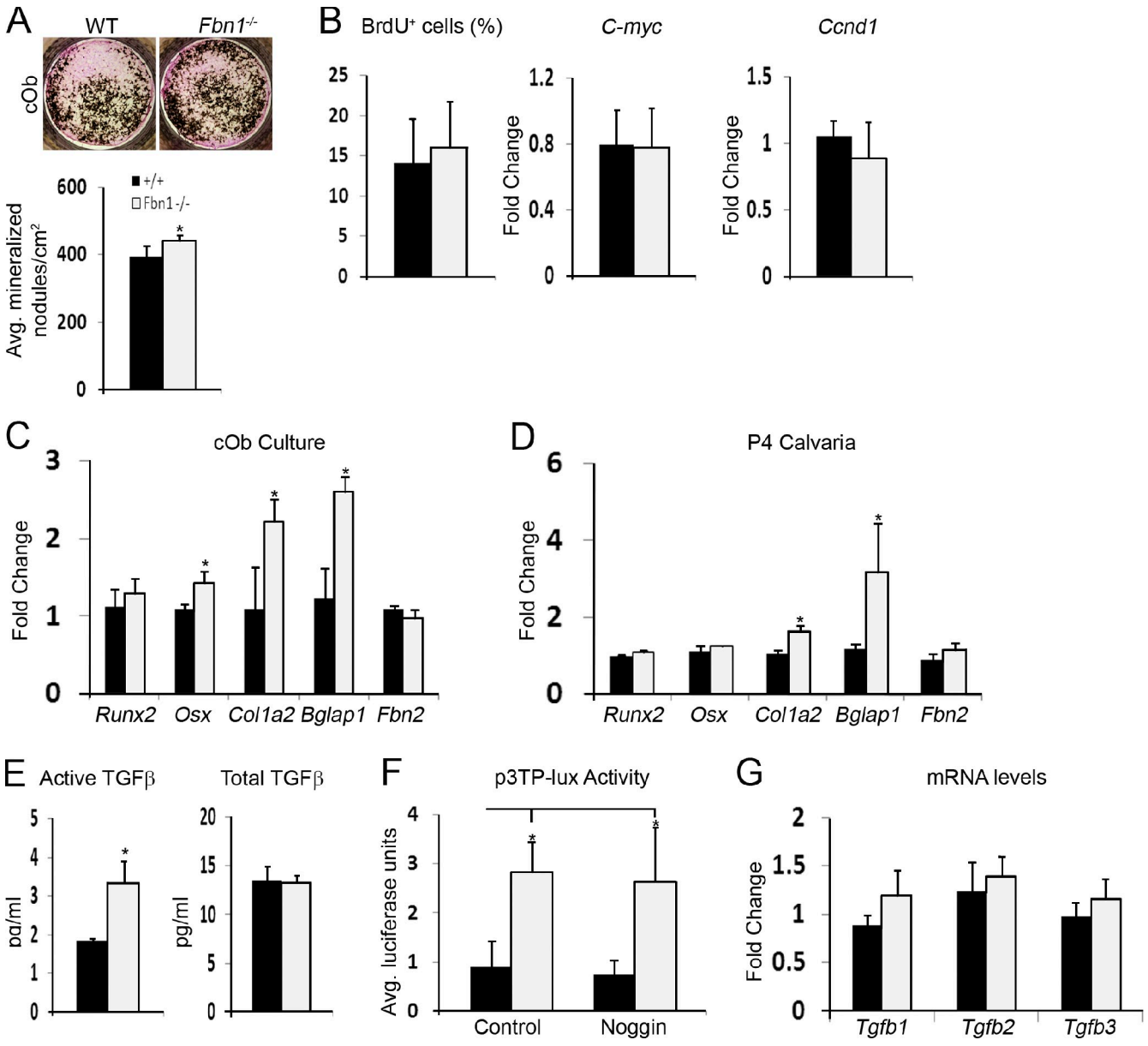

Figure 6. **Abnormally high TGF-β activity in differentiating *Fbn1*-null osteoblasts.** (A) Illustrative images of von Kossa–stained WT and *Fbn1*-null (*Fbn1*$^{-/-}$) cOb after 21 d of differentiation with histograms summarizing the number of mineralized nodules in each sample ($n = 5$). (B) Cell proliferation of WT and mutant cOb at day −3 of cell culture as assessed by BrdU incorporation and qPCR quantification of *C-myc* and *Ccnd1* transcripts ($n = 3$). (C and D) qPCR estimates of indicated transcripts in total RNA isolated from day 4 differentiating WT and mutant cOb cultures (C; $n = 4$) and from P4 WT and *Fbn1*$^{-/-}$ calvarial bones (D; $n = 3$). (E) TMLC bioassays ($n = 5$) measuring active TGF-β in WT or *Fbn1*-null cOb cultures (left) or total TGF-β in heat-activated conditioned media of the same cultures (right). (F) Transcriptional activity of p3TP-lux reporter plasmid transfected in WT or *Fbn1*-null cOb cultured in low serum with or without 1 µg/ml of noggin ($n = 3$). (G) qPCR estimates of *TGF-β* transcripts in WT and *Fbn2*-null cOb ($n = 3$). Error bars indicate mean ± SD, and asterisks indicate statistically significant differences ($P < 0.05$).

mineralization. Incidentally, little or no LTBP1-immunoreactive material in *Fbn2*-null cOb silenced for *Fbn1* supported prior evidence indicating that fibronectin and fibrillin assemblies are sequentially involved in incorporating LTBPs in the ECM (Fig. S2; Dallas et al., 2005).

Discussion

This study provides genetic validation for the long-held belief that sequential release of TGF-β and BMP ligands from the bone matrix contributes to the physiological maintenance of bone mass by balancing the pools of progenitor and mature osteoblasts (Mundy et al., 1995). It also identifies fibrillin microfibrils as the architectural elements of bone tissue that are principally involved in the storage of TGF-β and BMP complexes. Specifically, our experiments have shown that promiscuous TGF-β signaling is the cell-autonomous phenotype of primary osteoblast cultures derived from the bones of either *Fbn1*$^{-/-}$ or *Fbn2*$^{-/-}$ mice; they have established that unopposed TGF-β signaling in differentiating *Fbn2*-null osteoblasts selectively inhibits osterix and collagen I production; they have implied that fibrillin-1 deposition in the forming

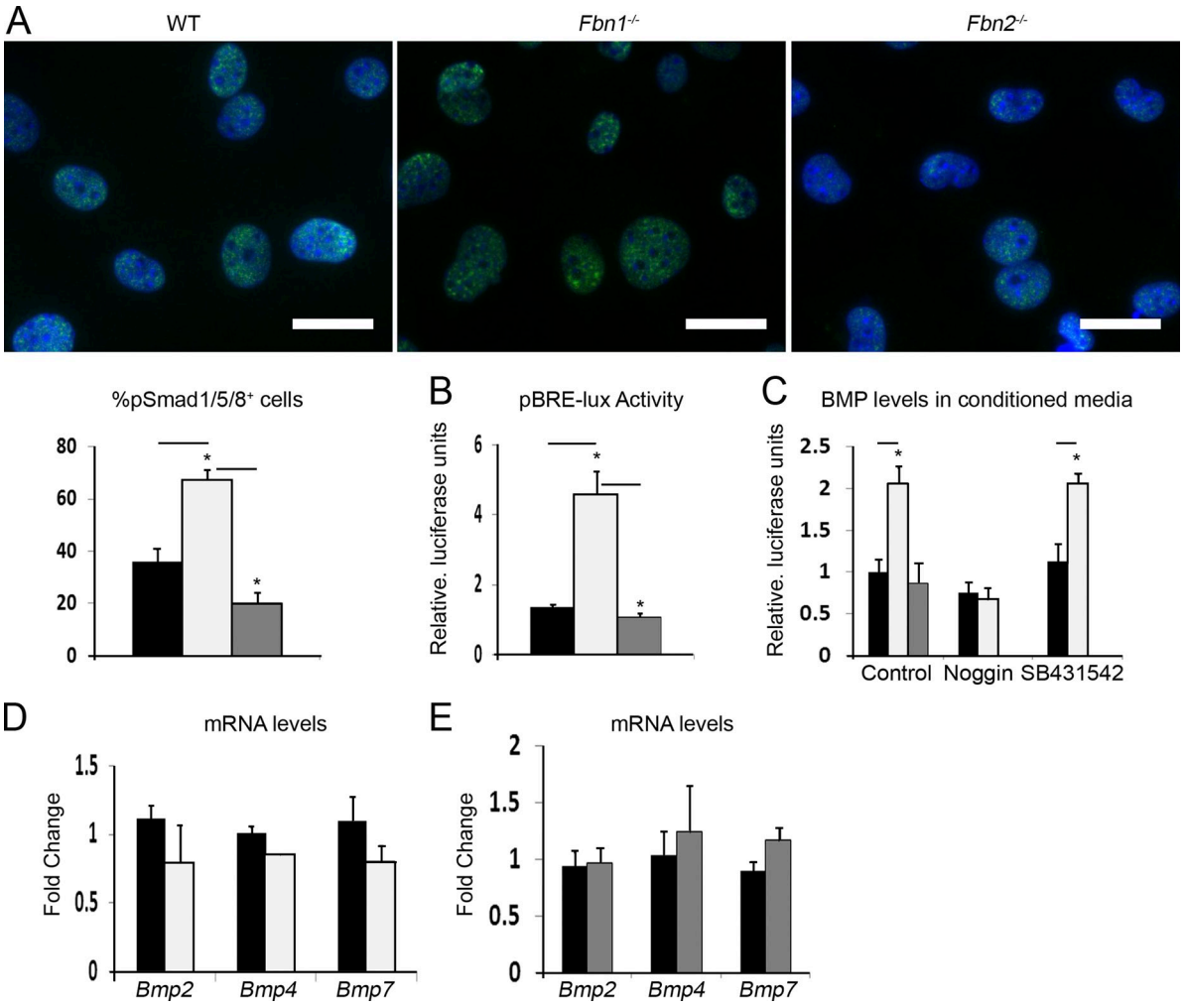

Figure 7. **Fibrillin-1 regulates BMP signaling in cultured osteoblasts.** (A) Immunodetection of nuclear pSmad1/5/8 accumulation in day 4 differentiating WT and *Fbn1*-null (*Fbn1*$^{-/-}$) and *Fbn2*-null (*Fbn2*$^{-/-}$) cOb cultured in low serum; nuclei are DAPI stained, and histograms summarize the percentage of pSmad1/5/8-positive nuclei in WT (black), *Fbn1*-null (white), or *Fbn2*-null (gray) cells (n = 3). Bars, 25 µm. (B) Transcriptional activity of pBRE-lux reporter plasmid in day 4 differentiating WT, *Fbn1*-null, and *Fbn2*-null cOb (n = 5). (C) C2Cl2BRA bioassay measuring BMP signaling in conditioned media from WT, *Fbn1*-null, and *Fbn2*-null cOb and from the first two cell cultures treated with either 1 µg/ml noggin or 1 µM SB431542 (n = 3). (D and E) qPCR estimates of *Bmp* transcripts in day 4 *Fbn1*$^{-/-}$ and *Fbn2*$^{-/-}$ cOb cultures, respectively (n = 3). Error bars indicate mean ± SD, and asterisks indicate statistically significant differences ($P < 0.05$).

bone matrix calibrates the threshold levels of local TGF-β and BMP signals during osteoblast maturation; and they have excluded that fibrillin microfibrils are required to constitute a mineralization-competent bone matrix (Fig. 9). Two broader conclusions can be drawn from this and our previous studies of microfibril mutant mice (Arteaga-Solis et al., 2001; Neptune et al., 2003; Carta et al., 2006; Habashi et al., 2006). First, fibrillin proteins control in a different manner and with discrete cellular outcomes the bioavailability of local TGF-β and BMP ligands during tissue formation and remodeling. Second, fibrillin assemblies impart contextual specificity to TGF-β and BMP signals by either concentrating the ligands at sites of intended function in the developing embryo (positive regulation, as exemplified by syndactyly in *Fbn2*$^{-/-}$ mice) or by restricting their gradual release during postnatal tissue modeling and remodeling (negative regulation, as exemplified by bone loss in *Fbn2*$^{-/-}$ mice and aortic aneurysm formation in *Fbn1* mutant mice).

Cell culture experiments have indicated that TGF-β and BMPs have both overlapping and opposing functions in bone formation. On the one hand, TGF-β stimulates the recruitment and proliferation of osteoblast progenitors but inhibits their terminal differentiation; and on the other hand, BMPs cooperate in the former process in addition to promoting osteogenic commitment of MSCs and osteoblast maturation (Alliston et al., 2008). However, albeit informative, these in vitro analyses have used exogenous stimulators or inhibitors of cell signaling and differentiation to infer the dynamics of locally released TGF-β and BMP signals during bone formation. For example, increased differentiation of C2C12 cells treated with BMP4 in the presence of an ALK5 inhibitor was interpreted to imply that endogenous TGF-β activity maintains normal bone mass by restricting the rate of osteoblast maturation through Smad-directed blockade of BMP signaling (Maeda et al., 2004). Similarly, genetic studies in mice have not directly interrogated the physiological contribution of matrix-bound TGF-β and BMP signals to bone modeling

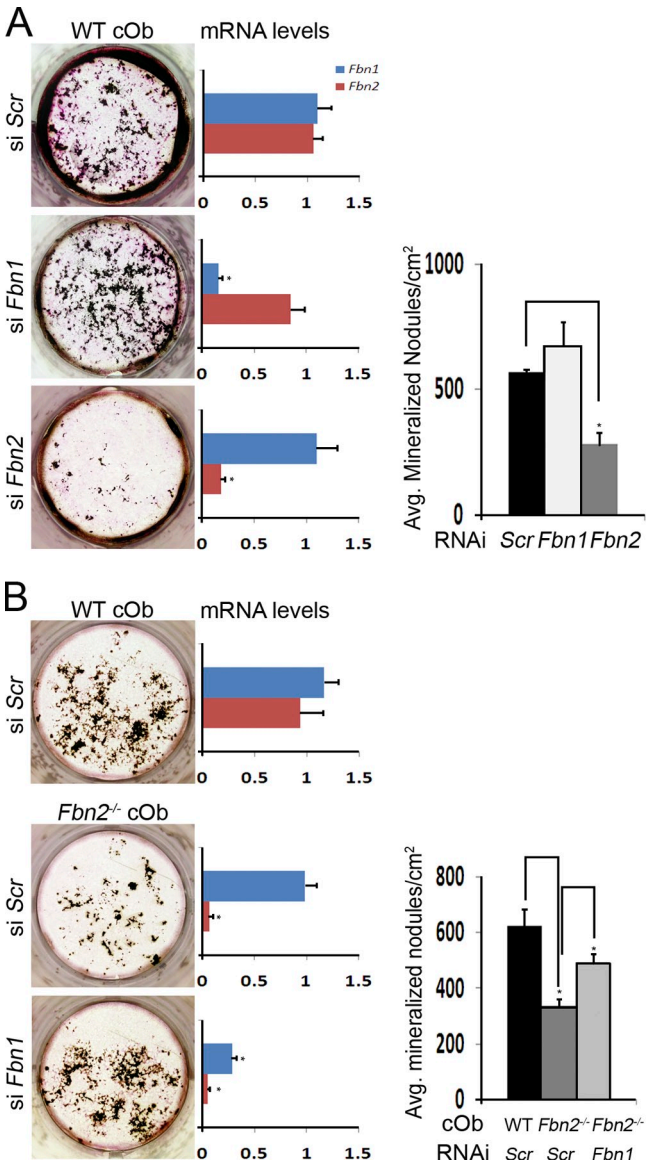

Figure 8. **Microfibrils are not a structural substrate for matrix mineralization.** (A) Illustrative von Kossa–stained WT cOb cultures in which *Fbn1* or *Fbn2* expression was silenced by RNAi with histograms on the immediate and far right showing the number of mineralized nodules and levels of indicated transcripts ($n = 3$), respectively. (B) Illustrative von Kossa–stained $Fbn2^{-/-}$ cOb cultures in which *Fbn1* was silenced with histograms on the immediate and far right, showing the number of mineralized nodules and levels of indicated transcripts, respectively ($n = 3$). Error bars indicate mean ± SD, and asterisks indicate statistically significant differences ($P < 0.05$).

and remodeling. In this respect, *Fbn*-null mice are the first animal models to yield unambiguous insights into the importance of the architectural matrix in modulating the local threshold levels of TGF-β and BMP signals during osteogenic differentiation.

Dynamic changes in ECM composition accompany and influence bone formation and mineralization. Collagens I and III, fibronectin, fibrillins, and large proteoglycans predominate in the matrix of osteoprogenitor cells; as preosteoblasts cease to proliferate and begin to differentiate, collagen I production increases substantially along with continued expression of fibrillins and secretion of small proteoglycans and matricellular proteins; once fully differentiated, osteoblasts produce osteocalcin

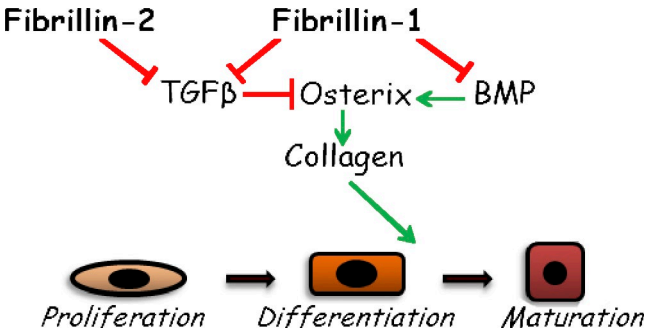

Figure 9. **Model of microfibril-mediated control of osteoblast maturation.** The scheme summarizes the distinct contributions of osteoblast-produced fibrillin-1 and fibrillin-2 microfibrils to osteogenic differentiation through the differential regulation of endogenous TGF-β and BMP signals that together calibrate the rate of bone formation.

(Ramirez, 2009). *Fbn2*-null osteoblasts are unable to assemble a mineralization-competent (collagen-rich) ECM, conceivably because promiscuous TGF-β activity delays the emergence of osterix-producing cells. Strong support for this conclusion includes in vivo cell-marking evidence showing that $Fbn2^{-/-}$ bones contain significantly fewer osteoblasts expressing *Col1a2* and cell culture data documenting the ability of *Fbn2*-null cOb to respond to TGF-β antagonism by reactivating *Osx* and *Col1a2* expression and resuming matrix mineralization. Along the same lines, others have reported that collagen production is repressed in $Osx^{-/-}$ mice (which lack differentiated osteoblasts; Wang et al., 2006) and stimulated in $p53^{-/-}$ mice (which display *Osx* up-regulation and high bone mass; Nakashima et al., 2002) and that a homozygous osterix mutation causes the collagen I–related condition osteogenesis imperfecta (Lapunzina et al., 2010). Increased latent TGF-β activation in *Fbn2*-null cOb has no apparent effect on cell proliferation. This somewhat surprising result is at least consistent with early in vitro analyses suggesting that exogenous TGF-β modulates cOb proliferation and collagen I production through different mechanisms, which are in part influenced by ligand concentration (Centrella et al., 1987). Our finding may also reflect the involvement of other signaling pathways that are stimulated as a result of promiscuous TGF-β activity and/or a structurally impaired ECM (Carta et al., 2009). Experimental context may also reconcile the unremarkable levels of *Runx2* mRNA observed in *Fbn2*-null cOb and the down-regulation of *Runx2* transcription previously reported in TGF-β–treated osteoblastic cells (Alliston et al., 2001).

Genetic interaction between fibrillin-2 and BMP7 in the forming mouse limbs originally predicted that extracellular microfibrils might control the bioavailability of other TGF-β family members (Arteaga-Solis et al., 2001). This prediction was subsequently corroborated by in vitro binding assays showing that the prodomain of several BMPs can bind with comparable affinity to the N-terminal regions of both fibrillin-1 and -2 (Sengle et al., 2008b). Additional analyses have led to the proposal that fibrillins may act as storage scaffolds that distribute, concentrate, and confer latency to BMPs conceivably in a stage and tissue-specific manner (Gregory et al., 2005; Sengle et al., 2008a). Our finding that maturing *Fbn1*-null osteoblast cultures are characterized by elevated BMP signaling, less matrix-bound BMP, and

normal *Bmp* mRNA levels is a very strong indication that fibrillin-1 microfibrils are indeed involved in sequestering BMP ligands in the bone matrix. Although heightened BMP signaling in *Fbn1*-null osteoblast cultures implies a context-specific mechanism that overrides the potential of fibrillin-2 to bind BMPs, it is still possible that fibrillin-2 might regulate BMP signaling earlier in osteoblastogenesis, as our study did not examine whether loss of *Fbn2* expression also impairs BMP-driven osteogenic commitment. In line with evidence of competitive LTBP and fibulin binding with fibrillin-1 (Ono et al., 2009), one or more ECM molecules may compete with BMP prodomains for the N termini of fibrillins at different stages of bone matrix assembly. A similar mechanism may also explain the reason why dysregulated BMP signaling is only seen in the forming digits of $Fbn2^{-/-}$ mice despite abundant fibrillin-1 production (Arteaga-Solis et al., 2001). It is also interesting to note that BMP signaling is low in the developing autopods of $Fbn2^{-/-}$ mice (as indicated by the syndactyly phenotype of $Fbn2^{+/-}$;$Bmp7^{+/-}$ mice; Arteaga-Solis et al., 2001) and high in the growing and remodeling bones of *Fbn1* mutant mice (as inferred by the BMP bioassay of *Fbn1*-null osteoblasts; Fig. 7 B). Collectively, these observations therefore support the hypothesis that extracellular microfibrils can control BMP bioavailability (and by extrapolation TGF-β bioavailability) both positively or negatively depending on developmental and physiological contexts and in a fibrillin-specific manner.

Although our findings have clearly established a causal relationship between fibrillin synthesis, matrix sequestration of TGF-β and BMP complexes, and progression of osteogenic differentiation, they have also raised several important new questions about the mechanisms underlying microfibril-mediated control of local TGF-β and BMP signaling. One question is whether latent TGF-β activation in a fibrillin-deficient state may reflect greater availability of the substrate to physiologically normal levels of activators, greater stimulation of activators by a structurally abnormal matrix or a combination of both mechanisms. A corollary to this question is whether or not the same mechanism of latent TGF-β activation operates in all affected tissues of fibrillin mutant mice. This information is particularly relevant to the clinical management of organ-specific manifestations in MFS. Indeed, although systemic inhibition of TGF-β signaling (via angiotensin receptor blockade) mitigates aortic aneurysm progression in MFS mice and patients (Habashi et al., 2006; Brooke, et al., 2008), preliminary data suggest that angiotensin receptor blockade therapy is ineffective to improve osteopenia in *Fbn1* mutant mice. As already noted, our study has left unresolved the important problem of how potentially equal interactions between fibrillins and TGF-β family members may impart spatiotemporal specificity to signaling events. This question is germane to the unresolved issue of how in vitro interactions between fibrillins and several other ECM proteins translate into the in vivo assembly of morphologically discrete macroaggregates. One attractive possibility is that cells may coordinate microfibril biogenesis at the plasma membrane with growth factor targeting to the ECM, as recent in vitro evidence suggests that fibronectin assemblies and cell surface receptors regulate both fibrillin polymerization and LTBP incorporation in the matrix (Dallas et al., 2005; Chen et al., 2007; Hubmacher et al., 2008; Sabatier et al., 2009). Moreover, the finding that fibrillin-2 molecules become gradually embedded within fibrillin-1 microfibrils during matrix maturation supports the notion that the dynamics of microfibril assembly may also determine the spatial distribution of signaling complexes within the ECM (Charbonneau et al., 2003, 2010). In this view, the tridimensional arrangement of fibrillin microfibrils may specify both the timely release and the optimal concentration of individual TGF-β family members and ultimately the proper behavior of resident cells, such as osteoblasts and osteoclasts during bone remodeling and fracture healing. In line with this postulate, our parallel study has implicated the fibrillins in modulating bone resorption as well through osteoblast-supported osteoclastogenesis (Nistala et al., 2010). In conclusion, this study has yielded important new insights into the extracellular control of local TGF-β and BMP signaling and implicitly, into the molecular pathophysiology of human diseases that are associated with primary or secondary deficits of the bone matrix.

Materials and methods

Histology and histomorphometry

$Fbn1^{-/-}$ and $Fbn2^{-/-}$ mice have been described previously (Arteaga-Solis et al., 2001; Carta, et al., 2006); transgenic mice *pOBCol2.3GFP* and *Osx-GFP::Cre* were provided by D. Rowe (University of Connecticut Health Center, Farmington, CT) and A. McMahon (Harvard University, Cambridge, MA), respectively (Kalajzic et al., 2005; Rodda and McMahon, 2006). Undecalcified vertebrae were embedded in methylmethacrylate, 7-µm-thick methylmethacrylate sections were stained with von Kossa, and 6-µm paraffin sections of femoral growth plates and calvariae were stained with hematoxylin/eosin and van Gieson, respectively, according to standard protocols. Lumbar vertebrae and femora of WT and mutant mice were isolated and scanned using a µCT system (eXplore Locus SP; GE Healthcare) with an isotropic voxel resolution of 9 µm in all three dimensions. All scans were performed using a density calibration phantom containing air, water, and a hydroxyapatite standard (SB3; Gammex RMI) to allow subsequent determinations of tissue mineral densities. Images were analyzed using data acquisition software (Evolver; GE Healthcare), image reconstruction software (Beam; GE Healthcare), and visualization and analysis software (Microview; GE Healthcare). To measure BFR, mice were injected with 25 mg/kg calcein 10 and 2 d before being sacrificed. Osteoblast number, BFR, and BV/TV were assessed using a microscope (DMLB; Leica) and attached color video camera (DXC-390; Sony) and the Osteomeasure analysis system (Osteometrics). Results were analyzed by an unpaired *t* test (Excel; Microsoft), assuming $P < 0.05$ as significant.

Primary osteoblast cultures

Standard protocols were used to prepare primary cultures of osteoblasts and MSCs from the calvariae or long bones of P2–4 or 7-wk-old mutant and WT mice, respectively (Bellows et al., 1986). Cells were cultured in α-MEM containing 10% FBS (HyClone) containing 1% penicillin/streptomycin (Invitrogen). Once confluent (day 0), cells were induced to differentiate by supplementing the culture medium with 50 µg/ml ascorbic acid and 10 mM β-glycerophosphate. The medium was changed every 3 d until day 21, when mineral deposits were visualized by von Kossa staining/van Geison counterstaining or by Alizarin red staining and quantified with MetaMorph imaging software (MDS Analytical Technologies). The same computer-aided quantification was used to examine cOb cultures harboring the *Osx-GFP::Cre* (at day 5 after induction) or *pOBCol2.3GFP* transgene (at day 17 after induction). In some experiments, culture media included 100 ng/ml rhBMP-2 (Wyeth Pharmaceuticals), 2 ng/ml rhTGF-β1 (R&D Systems), 1 µM SB431542 (Sigma-Aldrich) or 300 ng/ml neutralizing pan–TGF-β antibody (R&D Systems), and respective vehicle controls. Measurements of cell proliferation and viability and BrdU incorporation were performed according to standard protocols (Bonifacino et al., 2004). AP activity was measured using a commercial kit (AnaSpec). All cell images were acquired using a microscope (Eclipse TE200; Nikon) or a dissecting microscope (SMZ645; Nikon) connected to the aforementioned digital camera and processed using Photoshop (version 6.01; Adobe).

Statistical analyses were performed using an unpaired *t* test (Excel), assuming $P < 0.05$ as significant.

Immunoblots and immunocytochemistry

Osteoblasts were lysed in extraction buffer (50 mM Tris, 150 mM NaCl, 5 mM EDTA, 0.5% NP-40, and 0.1% Triton X-100) supplemented with 1 mM NaF, Na_2VO_3, 1 mM PMSF, and 1 µg/ml aprotonin, leupeptin, and pepstatin. Cell extracts were assayed for total protein content using the BCA kit (Thermo Fisher Scientific). Proteins extracts were resolved by 10% wt/vol SDS-PAGE and transferred onto Immobilon-P membranes (Millipore). Membranes were incubated first with antibody against mouse caspase-3, Smad2/3, pSmad2/3, and pSmad1/5/8 (1:1,000 dilution; Cell Signaling Technology) or β-actin (1:10,000 dilution; Sigma-Aldrich) and subsequently with biotin-labeled anti–rabbit IgG (1:25,000 dilution; Jackson ImmunoResearch Laboratories, Inc.) and HRP-conjugated streptavidin (Millipore). Nuclear accumulation of pSmads was evaluated by immunofluorescence staining of osteoblasts at day 4 after induction that were cultured in 2% FBS and subsequently fixed and incubated with antisera against pSmad2/3 or pSmad1/5/8 at 1:200 dilution and Alexa Fluor 488 or 594 anti–rabbit IgG secondary antibody (Invitrogen). Number of pSmad-positive nuclei was calculated on multiple fields and expressed as a percentage of total cells in the visual field. Likewise, osteoblast cultures at day 4 after induction were used for fibrillin-1, fibrillin-2, and LTBP-1 immunostaining as previously described (Charbonneau et al., 2003). Nuclei were visualized with DAPI staining. Images were acquired using Axiovision software on an imaging electron microscope (Axioplan; Carl Zeiss, Inc.) with the following objectives: Fluar 10×, Plan Apochromat 40×, Plan Neo Fluar 40×, and Plan Apochromat 63× (imaging medium: air for 10, 20, and 40×; and oil for 63×).

Cell transfections and RNAi

Osteoblasts were seeded the day before transfection at a density of 13,000 cells/cm^2 and cultured in 2% FBS. Cells were transiently cotransfected with 400 ng p3TP-lux or BRE-luc (provided by J. Massagué [Memorial Sloan-Kettering Cancer Center, New York, NY] and P. ten Dijke [Leiden University Medical Center, Leiden, Netherlands], respectively; Wrana et al., 1992; Logeart-Avramoglou et al., 2006) and 1 ng control plasmid SV40 Renilla luciferase (Promega) using Lipofectamine 2000 (Invitrogen). Luciferase assays were performed 24 h later and evaluated as previously described (Carta et al., 2009). WT or *Fbn2*-null cObs were transfected with 50 µM siRNA specific for *Fbn1*, *Fbn2* (Thermo Fisher Scientific), or *Alk5* (Invitrogen) using a nontargeting siRNA (Thermo Fisher Scientific) as a control (Carta et al., 2009). Total RNA was purified 2 d later and analyzed for gene silencing efficacy as described in the next paragraph. Parallel cell cultures were transfected once again 4 d later, and osteogenic media were added upon their reaching confluence. All experiments were performed using multiple independent samples and in triplicate. Values were analyzed using an unpaired *t* test, assuming $P < 0.05$ as significant.

RNA analyses

Total cellular or calvarial RNA was isolated using RNeasy Mini kit (QIAGEN). RNA concentration and purity were determined spectrophotometrically (NanoDrop; Thermo Fisher Scientific). Reverse transcription was performed with random hexamer primers (Invitrogen) and multiple temperature reverse transcription (AffinityScript; Agilent Technologies) using 1 µg total RNA as a template according to the manufacturer's instructions. The cDNAs were amplified using SYBR green supermix with ROX (6-carboxy-X-rhodamine; Fermentas) on a Mastercycler ep Realplex instrument (Eppendorf). *β-Actin* amplification was used as an internal reference for each sample. All qPCR primer sets were purchased from SuperArray Bioscience Corporation. Thermal cycling conditions were 95°C for 10 min followed by 40 cycles consisting of 95°C for 15-s denaturation, 60°C for 30-s annealing, and 72°C for 30-s extension. Comparative quantification was performed using multiple biological replicates that were analyzed in triplicate with the same untreated WT sample designated as the calibrator across different independent experimental runs. Statistical significance was evaluated by an unpaired *t* test, assuming significant association at $P < 0.05$ compared with control samples.

TGF-β and BMP bioassays

Cells for TGF-β and BMP bioassays were provided by D. Rifkin (New York University School of Medicine, New York, NY; Abe et al., 1994; Zilberberg et al., 2007). The former bioassays used either cocultures of TMLC and osteoblasts (to measure active TGF-β) or TMLC incubated in the presence of heat-activated conditioned media collected from osteoblast cultures (to measure total TGF-β). In both cases, cells were cultured at the density of 83,000 cells/cm^2 on 48-well plates in serum-free DME containing 0.1% BSA, and TGF-β activity was assessed 16 h later by measuring luciferase activity in cell lysates with a luminometer (TD-20; Turner Designs) as described previously (Abe et al., 1994). Resulting reporter gene values (normalized to cell number) were converted into amount of TGF-β (pg/ml) by comparing them with relative luciferase units of TMLC treated with increasing doses of rhTGF-β1. BMP bioassays were similarly performed by measuring relative luciferase units of C2C12BRA cells incubated with cOb-conditioned media as previously described (Zilberberg et al., 2007). To evaluate matrix-bound TGF-β, cells were washed twice with ice-cold PBS and removed using a lysis buffer (0.5% sodium deoxycholate and 10 mM Tris–HCl buffer, pH 8.0, containing 150 mM NaCl and 1% NP-40). Cell debris were removed with ice-cold PBS, and total TGF-β (activated by adding α-MEM containing 0.1% BSA and heating the tissue culture plate at 80°C for 15 min) was evaluated using the TLMC bioassay. To evaluate matrix-bound BMPs, cells were washed twice with PBS and removed using a lysis buffer (0.5% Triton X-100 and 20 mM ammonium hydroxide, pH 7.0). After removing cellular debris with ice-cold PBS, matrix-bound BMPs were solubilized into 10 mM Tris–HCl buffer containing 2 M urea, 2% SDS, and 10% glycerol, pH 6.8. Diluted samples were assayed using the BMP Quantikine kit (R&D Systems). Both bioassays were performed with multiple samples in triplicate and evaluated using an unpaired *t* test (Excel). Significant association was defined when $P < 0.05$ compared with control.

Surface plasmon resonance–binding assays

Binding analyses were performed using a BIAcoreX (BIAcore AB) and previously described recombinant LTBP1 (L1K), LTBP4 (L4K), and fibrillin-2 (rF86) peptides (Isogai et al., 2003; Ono et al., 2009). Peptides L1K and L4K were covalently coupled to CM5 sensor chips (research grade) using the amine coupling kit following the manufacturer's instructions (BIAcore AB). Binding responses caused by analyte interaction with the surface-coupled ligand were normalized by subtracting the background binding to plain control flow cells. Binding assays were performed at 25°C in 10 mM Hepes buffer, pH 7.4, containing 0.15 M NaCl, 2 mM EDTA, and 0.005% vol/vol P20 surfactant (HBS-EP buffer; BIAcore AB). Peptide rF86 was diluted in HBS-EP buffer and injected at several concentrations and different flow rates over immobilized LTBP peptides. The surface was regenerated with a pulse of 10 mM glycine, pH 1.7. Kinetic constants were calculated by nonlinear fitting (1:1 interaction model with mass transfer) to the association and dissociation curves according to the manufacturer's instructions (BIAevaluation software version 3.0; BIAcore AB). Apparent equilibrium dissociation constants (K_d) were calculated as the ratio of kd/ka.

Online supplemental material

Fig. S1 shows immunoblots of pSmad2/3 and pSmad1/5/8 proteins in fibrillin-deficient osteoblasts, collagen accumulation in *Fbn1*-null bones, AP and mineral nodule formation at different stages of *Fbn1*-null osteoblast maturation, and mineralization of and fibrillin-deficient osteoblast cultures treated with rhBMP2 or rhTGF-β1. Fig. S2 shows LTBP1 immunostaining in *Fbn2*-null cOb silenced for *Fbn1*. Online supplemental material is available at http://www.jcb.org/cgi/content/full/jcb.201003089/DC1.

We are indebted to Drs. Juan Massagué, Andrew McMahon, Daniel Rifkin, David Rowe, and Peter ten Dijke for sharing key reagents, Drs. Ernesto Canalis, Theresa Guise, Nicola Partridge, and Marian Young for experimental advices, and Drs. Harry Dietz and Daniel Rifkin for insightful discussions. We also thank Ms. Catherine Liu and Maria del Solar for excellent technical assistance and Ms. Karen Johnson for organizing the manuscript.

This work was supported by grants from the National Institutes of Health (AR42044 and AR49698), the Shriners Hospitals for Children, and the National Marfan Foundation.

Submitted: 19 March 2010
Accepted: 19 August 2010

References

Abe, M., J.G. Harpel, C.N. Metz, I. Nunes, D.J. Loskutoff, and D.B. Rifkin. 1994. An assay for transforming growth factor-β using cells transfected with a plasminogen activator inhibitor-1 promoter-luciferase construct. *Anal. Biochem.* 216:276–284. doi:10.1006/abio.1994.1042

Alliston, T., L. Choy, P. Ducy, G. Karsenty, and R. Derynck. 2001. TGF-β-induced repression of CBFA1 by Smad3 decreases cbfa1 and osteocalcin expression and inhibits osteoblast differentiation. *EMBO J.* 20:2254–2272. doi:10.1093/emboj/20.9.2254

Alliston, T., E. Piek, and R. Derynck. 2008. TGF-β family signaling in skeletal development, maintenance and disease. *In* The TGF-β Family.

R. Derynck and K. Miyazono, editors. Cold Spring Harbor Laboratory Press, Cold Spring Harbor, NY. 667–723.

Annes, J.P., J.S. Munger, and D.B. Rifkin. 2003. Making sense of latent TGFbeta activation. *J. Cell Sci.* 116:217–224. doi:10.1242/jcs.00229

Arteaga-Solis, E., B. Gayraud, S.Y. Lee, L. Shum, L.Y. Sakai, and F. Ramirez. 2001. Regulation of limb patterning by extracellular microfibrils. *J. Cell Biol.* 154:275–281. doi:10.1083/jcb.200105046

Bellows, C.G., J.E. Aubin, J.N. Heersche, and M.E. Antosz. 1986. Mineralized bone nodules formed in vitro from enzymatically released rat calvaria cell populations. *Calcif. Tissue Int.* 38:143–154. doi:10.1007/BF02556874

Bonifacino, J.S., M. Dasso, J.B. Harford, J. Lippincott-Schwartz, and K.M. Yamada. 2004. Short Protocols in Cell Biology Science: a Compendium of Methods from Current Protocols in Cell Biology. J. Wiley & Sons Inc., Hoboken, NJ. 826 pp.

Brooke, B.S., J.P. Habashi, D.P. Judge, N. Patel, B. Loeys, and H.C. Dietz III. 2008. Angiotensin II blockade and aortic-root dilation in Marfan's syndrome. *N. Engl. J. Med.* 358:2787–2795. doi:10.1056/NEJMoa0706585

Carta, L., L. Pereira, E. Arteaga-Solis, S.Y. Lee-Arteaga, B. Lenart, B. Starcher, C.A. Merkel, M. Sukoyan, A. Kerkis, N. Hazeki, et al. 2006. Fibrillins 1 and 2 perform partially overlapping functions during aortic development. *J. Biol. Chem.* 281:8016–8023. doi:10.1074/jbc.M511599200

Carta, L., S. Smaldone, L. Zilberberg, D. Loch, H.C. Dietz, D.B. Rifkin, and F. Ramirez. 2009. p38 MAPK is an early determinant of promiscuous Smad2/3 signaling in the aortas of fibrillin-1 (*Fbn1*)-null mice. *J. Biol. Chem.* 284:5630–5636. doi:10.1074/jbc.M806962200

Centrella, M., T.L. McCarthy, and E. Canalis. 1987. Transforming growth factor β is a bifunctional regulator of replication and collagen synthesis in osteoblast-enriched cell cultures from fetal rat bone. *J. Biol. Chem.* 262:2869–2874.

Charbonneau, N.L., B.J. Dzamba, R.N. Ono, D.R. Keene, G.M. Corson, D.P. Reinhardt, and L.Y. Sakai. 2003. Fibrillins can co-assemble in fibrils, but fibrillin fibril composition displays cell-specific differences. *J. Biol. Chem.* 278:2740–2749. doi:10.1074/jbc.M209201200

Charbonneau, N.L., C.D. Jordan, D.R. Keene, S. Lee-Arteaga, H.C. Dietz, D.B. Rifkin, F. Ramirez, and L.Y. Sakai. 2010. Microfibril structure masks fibrillin-2 in postnatal tissues. *J. Biol. Chem.* 285:20242–20251. doi:10.1074/jbc.M109.087031

Chen, Q., P. Sivakumar, C. Barley, D.M. Peters, R.R. Gomes, M.C. Farach-Carson, and S.L. Dallas. 2007. Potential role for heparan sulfate proteoglycans in regulation of transforming growth factor-β (TGF-β) by modulating assembly of latent TGF-β-binding protein-1. *J. Biol. Chem.* 282:26418–26430. doi:10.1074/jbc.M703341200

Dallas, S.L., P. Sivakumar, C.J.P. Jones, Q. Chen, D.M. Peters, D.F. Mosher, M.J. Humphries, and C.M. Kielty. 2005. Fibronectin regulates latent transforming growth factor-β (TGF β) by controlling matrix assembly of latent TGF β-binding protein-1. *J. Biol. Chem.* 280:18871–18880. doi:10.1074/jbc.M410762200

Ducy, P., R. Zhang, V. Geoffroy, A.L. Ridall, and G. Karsenty. 1997. Osf2/Cbfa1: a transcriptional activator of osteoblast differentiation. *Cell.* 89:747–754. doi:10.1016/S0092-8674(00)80257-3

Gregory, K.E., R.N. Ono, N.L. Charbonneau, C.L. Kuo, D.R. Keene, H.P. Bächinger, and L.Y. Sakai. 2005. The prodomain of BMP-7 targets the BMP-7 complex to the extracellular matrix. *J. Biol. Chem.* 280:27970–27980. doi:10.1074/jbc.M504270200

Habashi, J.P., D.P. Judge, T.M. Holm, R.D. Cohn, B.L. Loeys, T.K. Cooper, L. Myers, E.C. Klein, G. Liu, C. Calvi, et al. 2006. Losartan, an AT1 antagonist, prevents aortic aneurysm in a mouse model of Marfan syndrome. *Science.* 312:117–121. doi:10.1126/science.1124287

Hubmacher, D., E.I. El-Hallous, V. Nelea, M.T. Kaartinen, E.R. Lee, and D.P. Reinhardt. 2008. Biogenesis of extracellular microfibrils: Multimerization of the fibrillin-1 C terminus into bead-like structures enables self-assembly. *Proc. Natl. Acad. Sci. USA.* 105:6548–6553. doi:10.1073/pnas.0706335105

Isogai, Z., R.N. Ono, S. Ushiro, D.R. Keene, Y. Chen, R. Mazzieri, N.L. Charbonneau, D.P. Reinhardt, D.B. Rifkin, and L.Y. Sakai. 2003. Latent transforming growth factor β-binding protein 1 interacts with fibrillin and is a microfibril-associated protein. *J. Biol. Chem.* 278:2750–2757. doi:10.1074/jbc.M209256200

Judge, D.P., N.J. Biery, D.R. Keene, J. Geubtner, L. Myers, D.L. Huso, L.Y. Sakai, and H.C. Dietz. 2004. Evidence for a critical contribution of haploinsufficiency in the complex pathogenesis of Marfan syndrome. *J. Clin. Invest.* 114:172–181.

Kalajzic, I., A. Staal, W.P. Yang, Y. Wu, S.E. Johnson, J.H. Feyen, W. Krueger, P. Maye, F. Yu, Y. Zhao, et al. 2005. Expression profile of osteoblast lineage at defined stages of differentiation. *J. Biol. Chem.* 280:24618–24626. doi:10.1074/jbc.M413834200

Kang, J.S., C. Liu, and R. Derynck. 2009. New regulatory mechanisms of TGF-β receptor function. *Trends Cell Biol.* 19:385–394. doi:10.1016/j.tcb.2009.05.008

Karsenty, G., H.M. Kronenberg, and C. Settembre. 2009. Genetic control of bone formation. *Annu. Rev. Cell Dev. Biol.* 25:629–648. doi:10.1146/annurev.cellbio.042308.113308

Katagiri, T., T. Suda, and K. Miyazono. 2008. The bone morphogenetic proteins. *In* The TGF-β Family. R. Derynck and K. Miyazono, editors. Cold Spring Harbor Laboratory Press. Cold Spring Harbor, NY. 121–149.

Kitahama, S., M.A. Gibson, G. Hatzinikolas, S. Hay, J.L. Kuliwaba, A. Evdokiou, G.J. Atkins, and D.M. Findlay. 2000. Expression of fibrillins and other microfibril-associated proteins in human bone and osteoblast-like cells. *Bone.* 27:61–67. doi:10.1016/S8756-3282(00)00292-1

Lapunzina, P., M. Aglan, S. Temtamy, J.A. Caparrós-Martín, M. Valencia, R. Letón, V. Martínez-Glez, R. Elhossini, K. Amr, N. Vilaboa, and V.L. Ruiz-Perez. 2010. Identification of a frameshift mutation in Osterix in a patient with recessive osteogenesis imperfecta. *Am. J. Hum. Genet.* 87:110–114. doi:10.1016/j.ajhg.2010.05.016

Logeart-Avramoglou, D., M. Bourguignon, K. Oudina, P. Ten Dijke, and H. Petite. 2006. An assay for the determination of biologically active bone morphogenetic proteins using cells transfected with an inhibitor of differentiation promoter-luciferase construct. *Anal. Biochem.* 349:78–86. doi:10.1016/j.ab.2005.10.030

Maeda, S., M. Hayashi, S. Komiya, T. Imamura, and K. Miyazono. 2004. Endogenous TGF-β signaling suppresses maturation of osteoblastic mesenchymal cells. *EMBO J.* 23:552–563. doi:10.1038/sj.emboj.7600067

Mundy, G.R., B. Boyce, D. Hughes, K. Wright, L. Bonewald, S. Dallas, S. Harris, N. Ghosh-Choudhury, D. Chen, C. Dunstan, et al. 1995. The effects of cytokines and growth factors on osteoblastic cells. *Bone.* **17**(2, Suppl):71S–75S. doi:10.1016/8756-3282(95)00182-D

Murshed, M., D. Harmey, J.L. Millán, M.D. McKee, and G. Karsenty. 2005. Unique coexpression in osteoblasts of broadly expressed genes accounts for the spatial restriction of ECM mineralization to bone. *Genes Dev.* 19:1093–1104. doi:10.1101/gad.1276205

Nakashima, K., X. Zhou, G. Kunkel, Z. Zhang, J.M. Deng, R.R. Behringer, and B. de Crombrugghe. 2002. The novel zinc finger-containing transcription factor osterix is required for osteoblast differentiation and bone formation. *Cell.* 108:17–29. doi:10.1016/S0092-8674(01)00622-5

Neptune, E.R., P.A. Frischmeyer, D.E. Arking, L. Myers, T.E. Bunton, B. Gayraud, F. Ramirez, L.Y. Sakai, and H.C. Dietz. 2003. Dysregulation of TGF-β activation contributes to pathogenesis in Marfan syndrome. *Nat. Genet.* 33:407–411. doi:10.1038/ng1116

Nistala, H., S. Lee-Arteaga, S. Smaldone, G. Siciliano, and F. Ramirez. 2010. Extracellular microfibrils modulate osteoblast-supported osteoclastogenesis by restricting TGF beta stimulation of RANKL production. *J. Biol. Chem.* doi: 10.1074/jbc.M110.125328.

Ono, R.N., G. Sengle, N.L. Charbonneau, V. Carlberg, H.P. Bächinger, T. Sasaki, S. Lee-Arteaga, L. Zilberberg, D.B. Rifkin, F. Ramirez, et al. 2009. Latent transforming growth factor β-binding proteins and fibulins compete for fibrillin-1 and exhibit exquisite specificities in binding sites. *J. Biol. Chem.* 284:16872–16881. doi:10.1074/jbc.M809348200

Pereira, L., S.Y. Lee, B. Gayraud, K. Andrikopoulos, S.D. Shapiro, T. Bunton, N.J. Biery, H.C. Dietz, L.Y. Sakai, and F. Ramirez. 1999. Pathogenetic sequence for aneurysm revealed in mice underexpressing fibrillin-1. *Proc. Natl. Acad. Sci. USA.* 96:3819–3823. doi:10.1073/pnas.96.7.3819

Quondamatteo, F., D.P. Reinhardt, N.L. Charbonneau, G. Pophal, L.Y. Sakai, and R. Herken. 2002. Fibrillin-1 and fibrillin-2 in human embryonic and early fetal development. *Matrix Biol.* 21:637–646. doi:10.1016/S0945-053X(02)00100-2

Ramirez, F. 2009. Extracellular matrix in the skeleton. *In* The Skeletal System. O. Pourquié, editor. Cold Spring Harbor Laboratory Press, Cold Spring Harbor, NY. 341–353.

Ramirez, F., and E. Arteaga-Solis. 2008. Marfan syndrome and related disorders. *In* Primer on the Metabolic Bone Diseases and Disorders of Mineral Metabolism. Seventh Edition. C.J. Rosen, editor. American Society for Bone and Mineral Research Publications, Washington, D.C. 450–454.

Ramirez, F., and H.C. Dietz. 2007. Marfan syndrome: from molecular pathogenesis to clinical treatment. *Curr. Opin. Genet. Dev.* 17:252–258. doi:10.1016/j.gde.2007.04.006

Ramirez, F., and D.B. Rifkin. 2009. Extracellular microfibrils: contextual platforms for TGFbeta and BMP signaling. *Curr. Opin. Cell Biol.* 21:616–622. doi:10.1016/j.ceb.2009.05.005

Ramirez, F., and L.Y. Sakai. 2010. Biogenesis and function of fibrillin assemblies. *Cell Tissue Res.* 339:71–82. doi:10.1007/s00441-009-0822-x

Rodda, S.J., and A.P. McMahon. 2006. Distinct roles for Hedgehog and canonical Wnt signaling in specification, differentiation and maintenance of osteoblast progenitors. *Development.* 133:3231–3244. doi:10.1242/dev.02480

Roman-Roman, S., T. Garcia, A. Jackson, J. Theilhaber, G. Rawadi, T. Connolly, S. Spinella-Jaegle, S. Kawai, B. Courtois, S. Bushnell, et al. 2003. Identification of genes regulated during osteoblastic differentiation by

genome-wide expression analysis of mouse calvaria primary osteoblasts in vitro. *Bone.* 32:474–482. doi:10.1016/S8756-3282(03)00052-8

Rosen, V., and R.S. Thies. 1992. The BMP proteins in bone formation and repair. *Trends Genet.* 8:97–102.

Sabatier, L., D. Chen, C. Fagotto-Kaufmann, D. Hubmacher, M.D. McKee, D.S. Annis, D.F. Mosher, and D.P. Reinhardt. 2009. Fibrillin assembly requires fibronectin. *Mol. Biol. Cell.* 20:846–858. doi:10.1091/mbc.E08-08-0830

Sengle, G., R.N. Ono, K.M. Lyons, H.P. Bächinger, and L.Y. Sakai. 2008a. A new model for growth factor activation: type II receptors compete with the prodomain for BMP-7. *J. Mol. Biol.* 381:1025–1039. doi:10.1016/j.jmb.2008.06.074

Sengle, G., N.L. Charbonneau, R.N. Ono, T. Sasaki, J. Alvarez, D.R. Keene, H.P. Bächinger, and L.Y. Sakai. 2008b. Targeting of bone morphogenetic protein growth factor complexes to fibrillin. *J. Biol. Chem.* 283:13874–13888. doi:10.1074/jbc.M707820200

Shi, Y., and J. Massagué. 2003. Mechanisms of TGF-beta signaling from cell membrane to the nucleus. *Cell.* 113:685–700. doi:10.1016/S0092-8674(03)00432-X

Stein, G.S., J.B. Lian, and T.A. Owen. 1990. Bone cell differentiation: a functionally coupled relationship between expression of cell-growth- and tissue-specific genes. *Curr. Opin. Cell Biol.* 2:1018–1027. doi:10.1016/0955-0674(90)90151-4

ten Dijke, P., and H.M. Arthur. 2007. Extracellular control of TGFbeta signalling in vascular development and disease. *Nat. Rev. Mol. Cell Biol.* 8:857–869. doi:10.1038/nrm2262

Ulloa-Montoya, F., B.L. Kidder, K.A. Pauwelyn, L.G. Chase, A. Luttun, A. Crabbe, M. Geraerts, A.A. Sharov, Y. Piao, M.S.H. Ko, et al. 2007. Comparative transcriptome analysis of embryonic and adult stem cells with extended and limited differentiation capacity. *Genome Biol.* 8:R163. doi:10.1186/gb-2007-8-8-r163

Wang, X., H.Y. Kua, Y. Hu, K. Guo, Q. Zeng, Q. Wu, H.H. Ng, G. Karsenty, B. de Crombrugghe, J. Yeh, and B. Li. 2006. p53 functions as a negative regulator of osteoblastogenesis, osteoblast-dependent osteoclastogenesis, and bone remodeling. *J. Cell Biol.* 172:115–125. doi:10.1083/jcb.200507106

Wrana, J.L., L. Attisano, J. Cárcamo, A. Zentella, J. Doody, M. Laiho, X.F. Wang, and J. Massagué. 1992. TGF β signals through a heteromeric protein kinase receptor complex. *Cell.* 71:1003–1014. doi:10.1016/0092-8674(92)90395-S

Zhang, H., S.D. Apfelroth, W. Hu, E.C. Davis, C. Sanguineti, J. Bonadio, R.P. Mecham, and F. Ramirez. 1994. Structure and expression of fibrillin-2, a novel microfibrillar component preferentially located in elastic matrices. *J. Cell Biol.* 124:855–863. doi:10.1083/jcb.124.5.855

Zhang, H., W. Hu, and F. Ramirez. 1995. Developmental expression of fibrillin genes suggests heterogeneity of extracellular microfibrils. *J. Cell Biol.* 129:1165–1176. doi:10.1083/jcb.129.4.1165

Zilberberg, L., P. ten Dijke, L.Y. Sakai, and D.B. Rifkin. 2007. A rapid and sensitive bioassay to measure bone morphogenetic protein activity. *BMC Cell Biol.* 8:41. doi:10.1186/1471-2121-8-41